



## Structure-based virtual screening approach to the discovery of phosphoinositide 3-kinase alpha inhibitors

Hwangseo Park<sup>a,\*</sup>, Hwanho Choi<sup>a</sup>, Seunghee Hong<sup>b</sup>, Donghee Kim<sup>b</sup>, Dal-Seok Oh<sup>c</sup>, Sungwoo Hong<sup>b,\*</sup>

<sup>a</sup> Department of Bioscience and Biotechnology, Sejong University, 98 Kunja-Dong, Kwangjin-Ku, Seoul 143-747, Republic of Korea

<sup>b</sup> Department of Chemistry, Korea Advanced Institute of Science and Technology (KAIST), Daejeon 305-701, Republic of Korea

<sup>c</sup> Brain Disease Research Center, Korea Institute of Oriental Medicine, 483 Exporo, Yuseong-gu, Daejeon 305-811, Republic of Korea

### ARTICLE INFO

#### Article history:

Received 14 December 2010

Revised 3 February 2011

Accepted 4 February 2011

Available online 26 February 2011

#### Keywords:

Virtual screening

Docking

PI3K $\alpha$

Inhibitor

Anticancer agents

### ABSTRACT

Phosphoinositide 3-kinase alpha (PI3K $\alpha$ ) has proved to be an attractive target for the development of therapeutics for the treatment of cancer. Herein we report a successful application of the structure-based virtual screening to identify the novel inhibitors of PI3K $\alpha$ . These inhibitors have desirable physicochemical properties as a drug candidate and reveal a moderate potency with IC<sub>50</sub> values ranging from 20 to 40  $\mu$ M. Therefore, they deserve a consideration for further development by structure–activity relationship (SAR) studies to optimize the inhibitory activities. Structural features relevant to the stabilization of the newly identified inhibitors in the ATP-binding site of PI3K $\alpha$  are addressed in detail.

© 2011 Elsevier Ltd. All rights reserved.

Phosphoinositide 3-kinases (PI3Ks) play a pivotal role in intracellular trafficking through the phosphorylation at the 3-hydroxyl position of phosphatidylinositol 4,5-diphosphate (PIP2) to form phosphatidylinositol 3,4,5-triphosphate (PIP3). The resulting second messenger, PIP3, can regulate a variety of biological processes including the glucose metabolism and the growth, differentiation, survival, and migration of cells.<sup>1</sup> Aberrant upregulation of the PI3K pathway leads to an extraordinarily elevated PIP3 level and downstream activation of Akt, which has been known to be responsible for cancer, inflammation, immune disorders, and cardiovascular diseases.<sup>2</sup> Among the PI3K isoforms, the overexpression of PI3K $\alpha$  is observed in a broad spectrum of human cancers.<sup>3–6</sup> For instance, about 26% of breast cancers have been shown to stem from the PI3K $\alpha$ -deregulation. PI3K $\alpha$  pathway is thus one of the most frequently activated signaling pathways in oncogenic malignancies, and therefore the inhibition of PI3K has been considered to be a powerful approach for the treatment of cancer.

Accordingly, a great deal of efforts has been devoted to the discovery of PI3K $\alpha$  inhibitors with the aim to develop a novel anticancer medicine.<sup>7,8</sup> Among the reported inhibitors, wortmannin and LY294002 have been widely used to elucidate the functional role of PI3K and to inhibit the proliferation of cancer cells. However, their poor physicochemical properties and the high toxicity

associated with the nonselective kinase inhibition have made it difficult to be used in clinical application.<sup>9</sup> A number of ATP-competitive PI3K $\alpha$  inhibitors with improved physicochemical properties and selectivity have also been reported in the literature including BEZ235,<sup>10</sup> PI-103,<sup>11</sup> GDC-0941,<sup>12</sup> GSK2126458,<sup>13</sup> and PIK-75.<sup>14</sup>

In the present study, we identify the novel classes of PI3K $\alpha$  inhibitors by means of a structure-based drug design protocol involving the virtual screening with docking simulations and in vitro enzyme assay. The characteristic feature that discriminates our virtual screening approach from the others lies in the implementation of an accurate solvation model in calculating the binding free energy between PI3K $\alpha$  and the putative ligands, which would have an effect of increasing the hit rate in enzyme assay.<sup>15</sup> It will be shown that the docking simulations with the improved binding free energy function can be a useful tool for elucidating the activities of the identified inhibitors, as well as for enriching the chemical library with molecules that are likely to have desired biological activities.

Three dimensional (3D) coordinates in the X-ray crystal structure of PI3K $\alpha$  in the resting form (PDB code: 2RD0)<sup>16</sup> were selected as the receptor model in the virtual screening with docking simulations. After removing the solvent molecules, hydrogen atoms were added to each protein atom. A special attention was paid to assign the protonation states of the ionizable Asp, Glu, His, and Lys residues in the X-ray structure of PI3K $\alpha$ . The side chains of Asp and Glu residues were assumed to be neutral if one of their carboxylate oxygens pointed toward a hydrogen-bond accepting

\* Corresponding authors. Tel.: +82 2 3408 3766; fax: +82 2 3408 4334 (H. Park), tel.: +8242 350 2811; fax: +82 42 350 2810 (S.H.).

E-mail addresses: [dscho@kiom.re.kr](mailto:dscho@kiom.re.kr) (D.-S. Oh), [hongorg@kaist.ac.kr](mailto:hongorg@kaist.ac.kr) (S. Hong).

group including the backbone aminocarbonyl oxygen at a distance within 3.5 Å, a generally accepted distance limit for a hydrogen bond of moderate strength.<sup>17</sup> Similarly, the lysine side chains were assumed to be protonated unless the NZ atom was in proximity of a hydrogen-bond donating group. The same procedure was also applied to determine the protonation states of ND and NE atoms in His residues.

The docking library for PI3K $\alpha$  comprising about 240,000 compounds was constructed from the latest version of the chemical database distributed by Interbioscreen (<http://www.ibscreen.com>) containing approximately 477,000 synthetic and natural compounds. Prior to the virtual screening with docking simulations, they were filtrated on the basis of Lipinski's 'Rule of Five' to adopt only the compounds with the physicochemical properties of potential drug candidates<sup>18</sup> and without reactive functional group(s). All of the compounds included in the docking library were then subjected to the Corina program to generate their 3D atomic coordinates,<sup>19</sup> followed by the assignment of Gasteiger–Marsilli atomic charges.<sup>20</sup> We used the AutoDock program<sup>21</sup> in the virtual screening of PI3K $\alpha$  inhibitors because the outperformance of its scoring function over those of the others had been shown in several target proteins.<sup>22</sup> AMBER force field parameters were assigned for calculating the van der Waals interactions and the internal energy of a ligand as implemented in the original AutoDock program. Docking simulations with AutoDock were then carried out in the ATP-binding site of PI3K $\alpha$  to score and rank the compounds in the docking library according to their calculated binding affinities.

In the actual docking simulation of the compounds in the docking library, we used the empirical AutoDock scoring function improved by the implementation of a new solvation model for a compound. The modified scoring function has the following form:

$$\Delta G_{bind}^{aq} = W_{vdW} \sum_{i=1} \sum_{j>i} \left( \frac{A_{ij}}{r_{ij}^{12}} - \frac{B_{ij}}{r_{ij}^6} \right) + W_{hbond} \sum_{i=1} \sum_{j>i} E(t) \left( \frac{C_{ij}}{r_{ij}^{12}} - \frac{D_{ij}}{r_{ij}^{10}} \right) + W_{elec} \sum_{i=1} \sum_{j>i} \frac{q_i q_j}{\epsilon(r_{ij}) r_{ij}} + W_{tor} N_{tor} + W_{sol} \sum_{i=1} S_i \left( Occ_i^{max} - \sum_{j>i} V_j e^{-\frac{r_{ij}^2}{2\sigma^2}} \right) \quad (1)$$

where  $W_{vdW}$ ,  $W_{hbond}$ ,  $W_{elec}$ ,  $W_{tor}$ , and  $W_{sol}$  are the weighting factors of van der Waals, hydrogen bond, electrostatic interactions, torsional term, and desolvation energy of the inhibitors, respectively.  $r_{ij}$  represents the interatomic distance, and  $A_{ij}$ ,  $B_{ij}$ ,  $C_{ij}$ , and  $D_{ij}$  are related to the depths of the potential energy well and the equilibrium separations between the two atoms. The hydrogen bond term has an additional weighting factor,  $E(t)$ , representing the angle-dependent directionality. Cubic equation approach was applied to obtain the dielectric constant required in computing the interatomic electrostatic interactions between PI3K $\alpha$  and a ligand molecule.<sup>23</sup> In the

entropic term,  $N_{tor}$  is the number of  $sp^3$  bonds in the ligand. In the desolvation term,  $S_i$  and  $V_i$  are the solvation parameter and the fragmental volume of atom  $i$ ,<sup>24</sup> respectively, while  $Occ_i^{max}$  stands for the maximum atomic occupancy. In the calculation of molecular solvation free energy term in Eq. (1), we used the atomic parameters developed by Kang et al.<sup>25</sup> because those of the atoms other than carbon were unavailable. This modification of the solvation free energy term is expected to increase the accuracy in virtual screening because the underestimation of ligand solvation often leads to the overestimation of the binding affinity of a ligand with many polar atoms.<sup>15</sup>

Of the 240,000 compounds subject to the virtual screening with docking simulations, 100 top-scored compounds were selected as virtual hits. One ninety two of them were available from the compound supplier and were tested over PI3K $\alpha$  at 10  $\mu$ M concentration in a high-throughput binding assay (KINOMEScan, Ambit Biosciences).<sup>26</sup> Four compounds were discovered as hits with percent of control (POC) values less than 70, and were selected for the determination of  $IC_{50}$  values.<sup>27</sup> The chemical structures and the inhibitory activities of the newly identified inhibitors are shown in Figure 1 and Table 1, respectively. We note that compounds **1** and **2** possess quinazoline and quinazolin-4-one groups, respectively. These two-membered rings seem to serve as a mimic for the adenine group of ATP. To the best of our knowledge, compounds **1–4** have not been reported as PI3K inhibitors so far. As can be seen in Table 1, the four inhibitors reveal a moderate potency against PI3K $\alpha$  with the  $IC_{50}$  values of ranging from 20 to 40  $\mu$ M. Because these inhibitors are structurally diverse with a moderate inhibitory activity and good physicochemical properties as a drug candidate, they deserve a consideration for further development by structure–activity relationship (SAR) studies to optimize the inhibitory activities.

To obtain structural insight into the inhibitory mechanisms of the identified inhibitors of PI3K $\alpha$ , their binding modes in the ATP-binding site were investigated in a comparative fashion. Figure 2 shows the lowest-energy conformations of **1–4** in the ATP-binding site gorge of PI3K $\alpha$  calculated with the modified AutoDock program. The results of these docking simulations are self-consis-

**Table 1**  
 $IC_{50}$  values (in  $\mu$ M) of **1–4** against PI3K $\alpha$

Compounds	$IC_{50}$
<b>1</b>	23
<b>2</b>	28
<b>3</b>	40
<b>4</b>	40

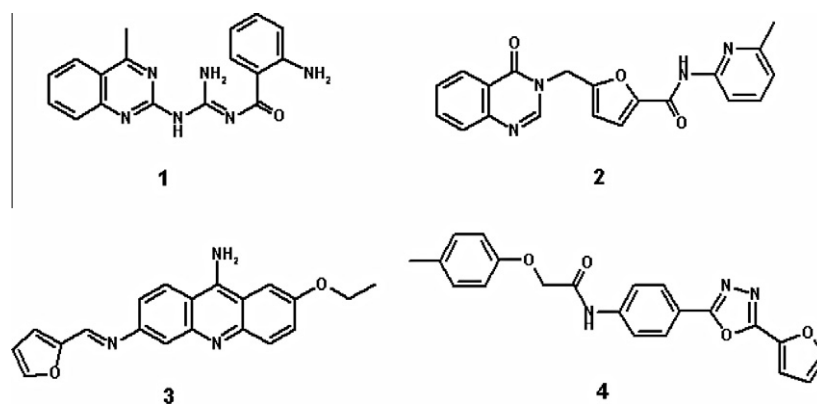


**Figure 1.** Chemical structures of the newly identified PI3K $\alpha$  inhibitors.

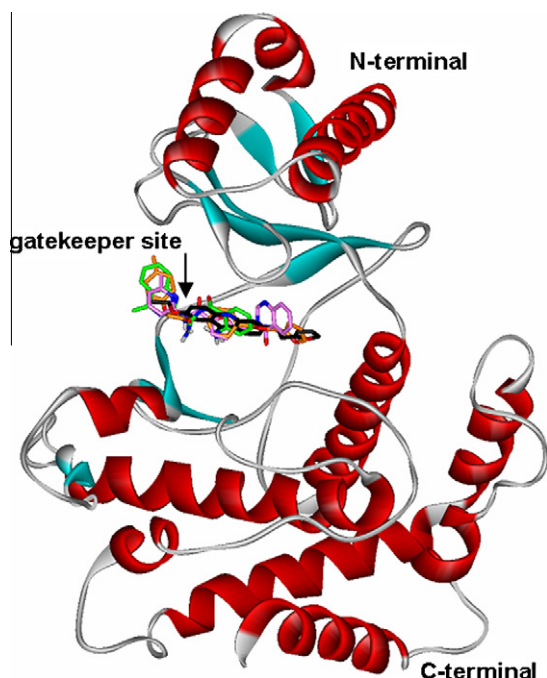


**Figure 2.** Comparative view of the binding modes of **1–4** in the ATP-binding site of PI3K $\alpha$ . Carbon atoms of **1**, **2**, **3**, and **4** are indicated in green, pink, black, and orange, respectively.

tent in the sense that the functional groups of similar chemical character are placed in similar ways with comparable interactions with the protein groups. As revealed by the superposition of their docked structures, for example, the hydrogen-bond donating groups of the inhibitors point toward the backbone groups at gatekeeper site of PI3K $\alpha$  with their hydrophobic groups being situated between the two loop structures at the top of C-terminal domain. In order to examine the possibility of the allosteric inhibition of PI3K $\alpha$  by the identified inhibitors, docking simulations were carried out with the grid maps for the receptor model so as to include the entire part of PI3K $\alpha$ . However, the binding configuration in which an inhibitor resides outside the ATP-binding site was not observed for any of the new inhibitors. These results support the possibility that the inhibitors would impair the catalytic activity of PI3K $\alpha$  through the specific binding in the ATP-binding site.

The calculated binding mode of **1** in the ATP-binding site of PI3K $\alpha$  is shown in Figure 3. It is noted that the  $-\text{NH}-$  groups attached to quinazoline and phenyl rings form a bifurcated hydrogen bond with the side-chain hydroxy group of Ser854. A stable hydrogen bond is also established between the central  $-\text{NH}_2$  group of the inhibitor and the backbone aminocarbonyl oxygen of Ser854. These three hydrogen bonds seem to play a role of anchor for binding of **1** because Ser854 resides in the middle of the ATP-binding site. The inhibitor **1** can be further stabilized in the ATP-binding site by the hydrophobic interactions of its nonpolar groups with the side chains of Trp780, Ile800, Ile848, Val851, Phe930, and Ile932. Judging from the overall structural features derived from docking simulations, the inhibitory activity of **1** is likely to stem from the multiple hydrogen bonds and hydrophobic interactions established simultaneously in the ATP-binding site. Considering the low molecular weight of  $\sim 320$ , **1** is expected to serve as a good inhibitor scaffold from which much more potent inhibitors can be derivatized.

Figure 4 shows the lowest-energy binding mode of **2** in the ATP-binding site of PI3K $\alpha$ . As in the PI3K $\alpha$ -**1** complex, the side-chain hydroxy group of Ser854 receives a hydrogen bond from the ami-

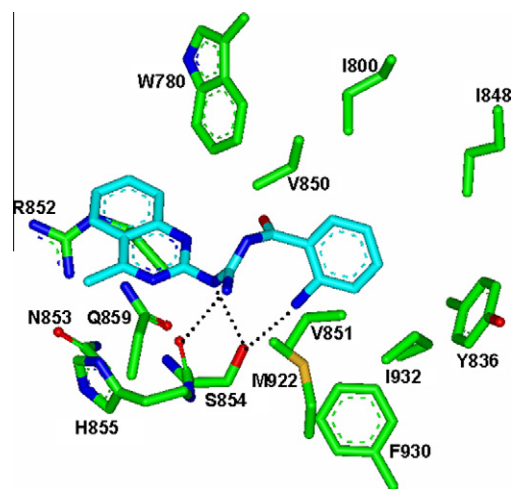


**Figure 3.** Calculated binding mode of **1** in the ATP-binding site of PI3K $\alpha$ . Carbon atoms of the protein and the ligand are indicated in green and cyan, respectively. Each dotted line indicates a hydrogen bond.

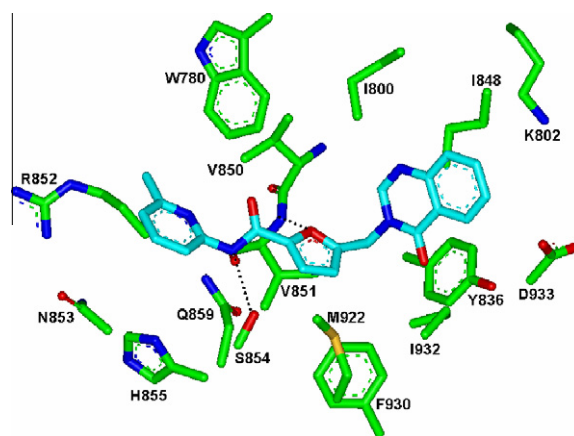


**Figure 4.** Calculated binding mode of **2** in the ATP-binding site of PI3K $\alpha$ . Carbon atoms of the protein and the ligand are indicated in green and cyan, respectively. Each dotted line indicates a hydrogen bond.

dic nitrogen of **2**. The formation of a hydrogen bond with Ser854 appears to be a common feature in the binding modes of the four inhibitors found in this study. However, the binding mode of **2** differs from that of **1** in that the backbone amidic nitrogen of Val851 should also play a role in stabilizing the inhibitor by donating a hydrogen bond to the furan group of **2**. It should also be noted that the number of hydrogen bonds decreases from three in the PI3K $\alpha$ -**1** to two in the PI3K $\alpha$ -**2** complex, which would have an effect of lowering the binding affinity. Hydrophobic interactions in the PI3K $\alpha$ -**2** complex are established in a similar way to that in the PI3K $\alpha$ -**1** complex: its pyridine, furan, and quinazolin-4-one rings are stabilized with the interactions with the side chains of Trp780, Ile800, Tyr836, Ile848, Val850, Val851, Phe930, and Ile932. However, the quinazolin-4-one ring of **2** is well accommodated in a small pocket comprising Ile800, Lys802, Tyr836, and Ile932, whereas the terminal aniline group of **1** resides at the entrance of the pocket. This indicates that the hydrophobic interactions in PI3K $\alpha$ -**2** complex should be stronger than that in PI3K $\alpha$ -**1** complex. Thus, the loss of one hydrogen bond seems to be compensated effectively by establishing the stronger hydrophobic interactions, which can be an explanation for the similar inhibitory activities of **1** and **2**.

In summary, we have identified four novel inhibitors of PI3K $\alpha$  by applying a computer-aided drug design protocol involving the structure-based virtual screening with docking simulations under consideration of the effects of ligand solvation in the scoring function. These inhibitors have desirable physicochemical properties as a drug candidate and reveal a moderate potency with IC<sub>50</sub> values ranging from 20 to 40  $\mu$ M. Therefore, each of the newly discovered inhibitors deserves consideration for further development by SAR studies to optimize the inhibitory activities. Detailed binding mode analyses with docking simulations show that the inhibitors can be stabilized in ATP-binding site by the simultaneous establishment of multiple hydrogen bonds and van der Waals contacts. Currently, we are planning to extend the structures by attaching additional groups of suitable shape, size, and polarity to enable into a back pocket (DFG-motif, gate keeper and catalytic lysine) with the expectation of combining high affinity for PI3K $\alpha$ .

## Acknowledgments

This work was supported by an intramural fund of Korea Institute of Oriental Medicine, Creative Research Program (K08142) and by National Research Foundation of Korea (NRF) funded by the Ministry of Education, Science and Technology (NRF-2010-001540 and 2010-0022179).

## References and notes

- Vanhaesebroeck, B.; Leever, S. J.; Khaterreh, A.; Timms, J.; Katso, R.; Driscoll, P. C.; Woscholski, R.; Parker, P. J.; Waterfield, M. D. *Annu. Rev. Biochem.* **2001**, *70*, 535.
- Cantley, L. C. *Science* **2002**, *296*, 1655.
- Samuels, Y.; Wang, Z.; Bardelli, A.; Silliman, N.; Ptak, J.; Szabo, S.; Yan, H.; Gazdar, A.; Powell, S. M.; Riggins, G. J.; Willson, J. K.; Markowitz, S.; Kinzler, K. W.; Vogelstein, B.; Velculescu, V. E. *Science* **2004**, *304*, 554.
- Parsons, D. W.; Wang, T.-L.; Samuels, Y.; Bardelli, A.; Cummins, J. M.; DeLong, L.; Silliman, N.; Ptak, J.; Szabo, S.; Willson, J. K.; Markowitz, S.; Kinzler, K. W.; Vogelstein, B.; Lengauer, C.; Velculescu, V. E. *Nature* **2005**, *436*, 792.
- Kang, S.; Bader, A. G.; Vogt, P. K. *Proc. Natl. Acad. Sci. U.S.A.* **2005**, *102*, 802.
- Fan, Q.-W.; Knight, A. A.; Goldenberg, D. D.; Yu, W.; Mostov, K. E.; Stokoe, D.; Shokat, K. M.; Weiss, W. A. *Cancer Cell* **2006**, *9*, 341.
- O'Brien, C.; Wallin, J. J.; Sampath, D.; Guhathakurta, D.; Savage, H.; Punnoose, E. A.; Guan, J.; Berry, L.; Prior, W. W.; Amler, L. C.; Belvin, M.; Friedman, L.; Lackner, M. *Clin. Cancer Res.* **2010**, *16*, 3670.
- Kong, D.; Yamori, T. *Curr. Med. Chem.* **2009**, *16*, 2836.
- Yap, T. A.; Garrett, M. D.; Walton, M. I.; Raynaud, F.; deBono, J. S.; Workman, P. *Curr. Opin. Pharmacol.* **2008**, *8*, 393.
- Stauffer, F.; Maira, S. M.; Furet, P.; Garcia-Echeverria, C. *Bioorg. Med. Chem. Lett.* **2008**, *18*, 1027.
- Hayakawa, M.; Kaizawa, H.; Moritomo, H.; Koizumi, T.; Ohishi, T.; Yamano, M.; Okada, M.; Ohta, M.; Tsukamoto, S.; Raynaud, F. I.; Workman, P.; Waterfield, M. D.; Parker, P. *Bioorg. Med. Chem. Lett.* **2007**, *17*, 2438.
- Folkes, A. J.; Ahmadi, K.; Alderton, W. K.; Alix, S.; Baker, S. J.; Box, G.; Chuckowree, I. S.; Clarke, P. A.; Depledge, P.; Eccles, S. A.; Friedman, L. S.; Hayes, A.; Hancox, T. C.; Kugendradas, A.; Lensun, L.; Moore, P.; Olivero, A. G.; Pang, J.; Patel, S.; Pergl-Wilson, G. H.; Raynaud, F. I.; Robson, A.; Saghir, N.; Salphati, L.; Sohal, S.; Ultsch, M. H.; Valenti, M.; Wallweber, H. J. A.; Wan, N. C.; Wiesmann, C.; Workman, P.; Zhyvoloup, A.; Zvelebil, M. J.; Shuttleworth, S. J. *J. Med. Chem.* **2008**, *51*, 5522.
- Knight, S. D.; Adams, N. D.; Burgess, J. L.; Chaudhari, A. M.; Darcy, M. G.; Donatelli, C. A.; Luengo, J. I.; Newlander, K. A.; Parrish, C. A.; Ridgers, L. H.; Sarpong, M. A.; Schmidt, S. J.; Van Aller, G. S.; Carson, J. D.; Diamond, M. A.; Elkins, P. A.; Gardiner, C. M.; Garver, E.; Gilbert, S. A.; Gontarek, R. R.; Jackson, J. R.; Kershner, K. L.; Luo, L.; Raha, K.; Sherk, C. S.; Sung, C.-M.; Sutton, D.; Tummino, P. J.; Wegrzyn, R. J.; Auger, K. R.; Dhanak, D. *Med. Chem. Lett.* **2010**, *1*, 39.
- Hayakawa, M.; Kawaguchi, K.; Kaizawa, H.; Koizumi, T.; Ohishi, T.; Yamano, M.; Okada, M.; Ohta, M.; Tsukamoto, S.; Raynaud, P. I.; Parker, P.; Workman, P.; Waterfield, M. D. *Bioorg. Med. Chem.* **2007**, *15*, 5837.
- Shoichet, B. K.; Leach, A. R.; Kuntz, I. D. *Proteins* **1999**, *34*, 4.
- Huang, C.-H.; Mandelker, D.; Schmidt-Kittler, O.; Samuels, Y.; Velculescu, V. E.; Kinzler, K. W.; Vogelstein, B.; Gabelli, S. B.; Amzel, L. M. *Science* **2007**, *318*, 1744.
- Jeffrey, G. A. *An Introduction to Hydrogen Bonding*; Oxford University Press: Oxford, 1997.
- Lipinski, C. A.; Lombardo, F.; Dominy, B. W.; Feeney, P. J. *Adv. Drug Deliv. Rev.* **1997**, *23*, 3.
- Gasteiger, J.; Rudolph, C.; Sadowski, J. *Tetrahedron Comp. Method* **1990**, *3*, 537.
- Gasteiger, J.; Marsili, M. *Tetrahedron* **1980**, *36*, 3219.
- Morris, G. M.; Goodsell, D. S.; Halliday, R. S.; Huey, R.; Hart, W. E.; Belew, R. K.; Olson, A. J. *J. Comput. Chem.* **1998**, *19*, 1639.
- Park, H.; Lee, J.; Lee, S. *Proteins* **2006**, *65*, 549.
- Park, H.; Jeon, J. H. *Phys. Rev. E* **2007**, *75*, 021916.
- Stouten, P. F. W.; Frömmel, C.; Nakamura, H.; Sander, C. *Mol. Simul.* **1993**, *10*, 97.
- Kang, H.; Choi, H.; Park, H. *J. Chem. Inf. Model.* **2007**, *47*, 509.
- Fabian, M. A.; Biggs, W. H., III; Treiber, D. K.; Atteridge, C. E.; Azimioara, M. D.; Bendetti, M. G.; Carter, T. A.; Ciceri, P.; Edeen, P. T.; Floyd, M.; Ford, J. M.; Galvin, M.; Gerlach, J. L.; Grotzfeld, R. M.; Herrgard, S.; Insko, D. E.; Insko, M. A.; Lai, A. G.; Lelias, J.-M.; Mehta, S. A.; Milanov, Z. V.; Velasco, A. M.; Wodicka, L. M.; Patel, H. K.; Zarrinkar, P. P.; Lockhart, D. J. *Nat. Biotechnol.* **2005**, *23*, 329.
- Full IC<sub>50</sub> values for PI3K $\alpha$  were determined using PI3-Kinase Glo kit (Promega-inc).